ISSN 0021-8944, Journal of Applied Mechanics and Technical Physics, 2019, Vol. 60, No. 6, pp. 996–1004. © Pleiades Publishing, Ltd., 2019.
Original Russian Text © S. Ahmad, M. Ashraf, K. Ali.

NUMERICAL SIMULATION OF VISCOUS DISSIPATION IN A MICROPOLAR FLUID FLOW THROUGH A POROUS MEDIUM

S. Ahmad[a], M. Ashraf[a,*], and K. Ali[b]

UDC 532.5

Abstract: Taking into account the effect of viscous dissipation in the energy equation, we numerically explore the flow of an incompressible micropolar fluid with heat and mass transfer through a resistive porous medium between plane channel walls. By exploiting a similarity transformation, the governing partial differential equations are transformed into a system of nonlinear coupled ordinary differential equations, which are solved numerically for various problem parameters by means of quasi-linearization. It is found that the effect of viscous dissipation is to increase the heat and mass transfer rate at both the lower and upper walls of the channel.

Keywords: viscous dissipation, micropolar fluid, porous medium, quasi-linearization.

DOI: 10.1134/S0021894419060038

INTRODUCTION

Micropolar fluids consist of microstructured polymeric additives and are exemplified as non-Newtonian fluids. The whirling microconstituents of micropolar fluids agitate the hydrodynamics of the fluid flow, and this mechanism provides a basis for successful implementation of micropolar fluids in modern engineering and biotechnology. Micropolar fluids can describe the flow behavior of ferroliquids, colloidal fluids, polymeric materials, exotic lubricants, animal blood, paints, etc. Eringen [1, 2] was the pioneer in introducing the theory of micropolar fluids. The micropolar fluid flow model involves an additional transport equation obeying the principle of conservation of local angular momentum. This model was further developed by Ariman et al. [3, 4] who also provided examples of applications of micropolar fluids.

Combined effects of heat and mass transfer in fluid flow problems have practical implementations in biotechnology and geophysics (e.g., air circulation in the respiratory system, binary gas diffusion, drying of porous solid surfaces, combustion process in rocket motors, production of ceramics and synthesis materials, etc). During the last few decades, the micropolar fluid flow, heat and mass transfer through channels were intensely studied. Ziabakhsh and Domairry [5] interpreted a micropolar fluid flow and mass transfer through a porous channel by using the homotopy analysis technique. A micropolar fluid flow through a channel having permeable walls was examined by Mirzaaghaian and Ganji [6] by using the differential transformation method. They concluded that the temperature and concentration are only slightly affected by the Reynolds number. Ali and Ashraf [7] numerically explored a micropolar fluid flow and heat transfer in a channel by assuming that one wall of the channel is shrinking and the other wall is stationary. Fakour et al. [8] studied a micropolar fluid flow by the least squares method combined with

[a]Centre for Advanced Studies in Pure and Applied Mathematics, Bahauddin Zakariya University, Multan, 60800 Pakistan; sohailkhan1058@gmail.com; *muhammadashraf@bzu.edu.pk. [b]Department of Basic Sciences and Humanities, Muhammad Nawaz Sharif University of Engineering and Technology, Multan, 60000, Pakistan; kshifali_381@yahoo.com. Translated from Prikladnaya Mekhanika i Tekhnicheskaya Fizika, Vol. 60, No. 6, pp. 25–34, November–December, 2019. Original article submitted April 1, 2019; revision submitted April 1, 2019; accepted for publication June 24, 2019.

*Corresponding author.

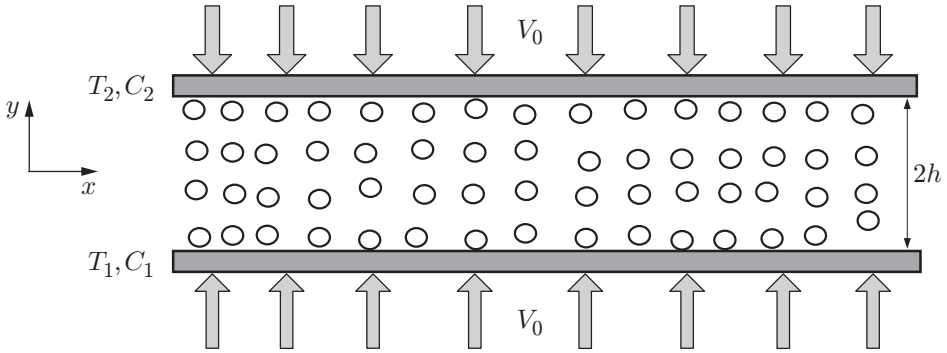

Fig. 1. Geometry of the problem.

the fourth-order Runge–Kutta technique. Mirgolbabaee et al. [9] solved the problem formulated in [8] by using Akbari Ganji's method, while Sheikholeslami et al. [10] solved the same problem by using the homotopy perturbation method; The results were equated to those obtained by the fourth-order Runge–Kutta scheme. Xinhui Si et al. [11] solved this problem with expanding or contracting walls of a porous channel by exploiting the homotopy analysis method. Nwabuzor et al. [12] considered a magnetohydrodynamic micropolar fluid flow in a porous medium. Based on the results of numerical simulations of Ashraf et al. [13] and Shrestha and Terrill [14], it was found that the skin friction coefficient on the channel walls for micropolar fluids is smaller than that for Newtonian fluids.

The purpose of the present study is to analyze the numerical solutions for heat and mass transfer in a viscous incompressible micropolar fluid flow through a resistive porous medium in a channel with plane walls.

1. PHYSICAL MODEL

We consider a steady laminar flow of a viscous incompressible micropolar fluid through a channel filled with a resistive porous medium. The temperature and solute concentration at the lower channel wall are denoted by T_1 and C_1. The upper channel wall has the temperature T_2 and the solute concentration C_2 (Fig. 1). The channel walls are parallel to the x axis and have the coordinates $y = \pm h$ ($2h$ is the channel width).

The differential equations governing the flow, heat transfer, and concentration have the form

$$\frac{\partial u}{\partial x} + \frac{\partial v}{\partial y} = 0;$$

$$\rho\Big(u\,\frac{\partial u}{\partial x} + v\,\frac{\partial u}{\partial y}\Big) = -\frac{\partial p}{\partial x} + (\mu + k)\Big(\frac{\partial^2 u}{\partial x^2} + \frac{\partial^2 u}{\partial y^2}\Big) - \frac{\mu + k}{k^*}\,u + k\,\frac{\partial N}{\partial y},$$

$$\rho\Big(u\,\frac{\partial v}{\partial x} + v\,\frac{\partial v}{\partial y}\Big) = -\frac{\partial p}{\partial y} + (\mu + k)\Big(\frac{\partial^2 v}{\partial x^2} + \frac{\partial^2 v}{\partial y^2}\Big) - \frac{\mu + k}{k^*}\,v - k\,\frac{\partial N}{\partial x},$$

$$\rho\Big(u\,\frac{\partial N}{\partial x} + v\,\frac{\partial N}{\partial y}\Big) = -\frac{k}{j}\Big(2N + \frac{\partial u}{\partial x} - v\,\frac{\partial v}{\partial y}\Big) + \frac{\mu_s}{j}\Big(\frac{\partial^2 N}{\partial x^2} + \frac{\partial^2 N}{\partial y^2}\Big), \tag{1}$$

$$\rho C_p\Big(u\,\frac{\partial T}{\partial x} + v\,\frac{\partial T}{\partial y}\Big) = k_1\,\frac{\partial^2 T}{\partial y^2} + \mu\Big(\frac{\partial u}{\partial y}\Big)^2,$$

$$u\,\frac{\partial C}{\partial x} + v\,\frac{\partial C}{\partial y} = D^*\,\frac{\partial^2 C}{\partial y^2},$$

where x and y the coordinates of the axes along and across the channel, u and v are the velocity components in the x and y directions, respectively, ρ is the fluid density, μ is the dynamic viscosity, N is the angular velocity, p is the pressure, k^* is the Darcy permeability, C_p is the specific heat, k is the vortex viscosity, j is the microinertia,

$\mu_s = \mu + k/2$ is the microrotation viscosity, k_1 is the thermal conductivity, D^* is the molecular diffusivity, T is the temperature, and C is the concentration of the fluid.

The following boundary conditions are imposed at $y = \pm h$:

$$y = -h: \qquad u = 0, \quad v = -v_0, \quad N = 0, \quad T = T_1, \quad C = C_1,$$

$$y = h: \qquad u = 0, \quad v = v_0, \quad N \to 0, \quad T \to T_2, \quad C \to C_2.$$

Let us introduce the similarity transformations

$$\eta = \frac{y}{h}, \quad \psi = -v_0 x f(\eta), \quad N = \frac{v_0 x}{h^2}\, g(\eta), \quad \theta(\eta) = \frac{T - T_2}{T_1 - T_2}, \quad \varphi(\eta) = \frac{C - C_2}{C_1 - C_2}, \tag{2}$$

where $T_2 = T_1 - Ax$, $C_2 = C_1 - Bx$, and A and B are constants. Using these similarity variables (2) in Eqs. (1), we obtain the set of ordinary differential equations

$$\begin{gathered}(1 + C_1) f^{\mathrm{iv}} - \mathrm{Re}\, f f''' + \mathrm{Re}\, f' f'' - \varepsilon(1 + C_1) f'' - C_1 g'' = 0, \\ C_2 g'' + C_1 (f'' - 2g) - C_3\, \mathrm{Re}\, (f g' - f' g) = 0;\end{gathered} \tag{3}$$

$$\theta'' + \mathrm{Pe}_h(\mathrm{Ec}\, f''^2 + f'\theta - f\theta') = 0, \qquad \varphi'' + \mathrm{Pe}_m(f'\varphi - f\varphi') = 0 \tag{4}$$

with the boundary conditions

$$\begin{gathered}\eta = -1: \qquad f = 1, \quad f' = 0, \quad g = 0, \quad \theta = 1, \quad \varphi = 1, \\ \eta = 1: \qquad f = -1, \quad f' = 0, \quad g = 0, \quad \theta = 0, \quad \varphi = 0.\end{gathered} \tag{5}$$

The constants involved in Eqs. (3) and (4) are

$$\mathrm{Re} = \frac{v_0}{v}\, h, \quad C_1 = \frac{k}{\mu}, \quad C_2 = \frac{\mu_s}{\mu h^2}, \quad C_3 = \frac{j}{h^2}, \quad \varepsilon = \frac{h^2}{k^*},$$

$$\mathrm{Pr} = \frac{v\rho C_p}{k_1}, \quad \mathrm{Pe}_h = \mathrm{PrRe}, \quad \mathrm{Ec} = \frac{v_0^2 x v}{h^3 C_p}, \quad \mathrm{Sc} = \frac{\nu}{D^*}, \quad \mathrm{Pe}_m = \mathrm{ScRe}.$$

Here Re is the Reynolds number, C_1 is the vortex viscosity parameter, C_2 is the spin-gradient viscosity parameter, C_3 is the microinertia density parameter, ε is the porosity parameter, Pr is the Prandtl number, Pe_h and Pe_m are the Peclet numbers for the heat and mass diffusion, respectively, Ec is the Eckert number, and Sc is the Schmidt number. The parameters of primary interest are the local Nusselt number and the Sherwood number:

$$\mathrm{Nu}_x = \frac{q'' x}{(T_1 - T_2) k_1}\Big|_{y=-h} = -\theta'(-1), \qquad \mathrm{Sh}_x = \frac{m'' x}{(C_1 - C_2) k_1}\Big|_{y=-h} = -\varphi'(-1)$$

(q'' and m'' are the local heat and mass fluxes, respectively).

2. QUASI-LINEARIZATION METHOD

We use the quasi-linearization method by assembling the sequences of the functions $\{f^{(k)}\}$, $\{g^{(k)}\}$, $\{\theta^{(k)}\}$, and $\{\varphi^{(k)}\}$, which converge to the numerical solution of system (3), (4). To construct the sequence $\{f^{(k)}\}$, we linearize Eq. (3). Let us define the function G as

$$G(f, f', f'', f''', f^{\mathrm{iv}}) = (1 + C_1) f^{\mathrm{iv}} - \mathrm{Re} f f''' + \mathrm{Re} f' f'' - \varepsilon(1 + C_1) f''.$$

Expanding the function G into the Taylor series and retaining only the first-order terms, we find

$$G(f^{(k)}, f^{(k)\prime}, f^{(k)\prime\prime}, f^{(k)\prime\prime\prime}, f^{(k)\mathrm{iv}}) + (f^{(k+1)} - f^{(k)}) \frac{\partial G}{\partial f^{(k)}} + (f^{(k+1)\prime} - f^{(k)\prime}) \frac{\partial G}{\partial f^{(k)\prime}} +$$

$$+ (f^{(k+1)\prime\prime} - f^{(k)\prime\prime}) \frac{\partial G}{\partial f^{(k)\prime\prime}} + (f^{(k+1)\prime\prime\prime} - f^{(k)\prime\prime\prime}) \frac{\partial G}{\partial f^{(k)\prime\prime\prime}} + (f^{(k+1)\mathrm{iv}} - f^{(k)\mathrm{iv}}) \frac{\partial G}{\partial f^{(k)\mathrm{iv}}} = 0.$$

After simplification, we obtain

$$(1+C_1)f^{(k+1)\mathrm{iv}} - \mathrm{Re}f^{(k)}f^{(k+1)'''} + [\mathrm{Re}f^{(k)'} - \varepsilon(1+C_1)]f^{(k+1)''}$$

$$+ \mathrm{Re}f^{(k)''}f^{(k+1)'} - \mathrm{Re}f^{(k)'''}f^{(k+1)} = \mathrm{Re}\,(f^{(k)'}f^{(k)''} - f^{(k)}f^{(k)'''}) + C_1 g^{(k)''}. \tag{6}$$

Replacing the derivatives in the ordinary differential equations (6) by central differences, we obtain the equations for determining the sequence $\{f^{(k)}\}$:

$$[(1+C_1) + h\mathrm{Re}f_i^{(k)}]f_{i-2}^{(k+1)} + [-4(1+C_1) - 2h\mathrm{Re}f_i^{(k)} + 0.5h\mathrm{Re}\,(f_{i+1}^{(k)} - f_{i-1}^{(k)})$$

$$- \varepsilon(1+C_1)h^2 - 0.5h\mathrm{Re}\,(f_{i+1}^{(k)} - 2f_i^{(k)} + f_{i-1}^{(k)})]f_{i-1}^{(k+1)} + [6(1+C_1) + h\mathrm{Re}\,(f_{i+1}^{(k)} - f_{i-1}^{(k)})$$

$$+ 2\varepsilon(1+C_1)h^2 - h\mathrm{Re}\,(f_{i+2}^{(k)} - 2f_{i+1}^{(k)} + 2f_{i-1}^{(k)} - 2f_{i-2}^{(k)})]f_i^{(k+1)}$$

$$+ [-4(1+C_1) + 2h\mathrm{Re}f_i^{(k)} + 0.5h\mathrm{Re}\,(f_{i+1}^{(k)} - f_{i-1}^{(k)}) - \varepsilon(1+C_1)h^2$$

$$+ 0.5h\mathrm{Re}\,(f_{i+1}^{(k)} - 2f_i^{(k)} + f_{i-1}^{(k)})]f_{i+1}^{(k+1)} + [(1+C_1) - h\mathrm{Re}f_i^{(k)}]f_{i+2}^{(k+1)}$$

$$= 0.5h\mathrm{Re}\,(f_{i+1}^{(k)} - f_{i-1}^{(k)})(f_{i+1}^{(k)} - 2f_i^{(k)} + f_{i-1}^{(k)}) - h\mathrm{Re}f_i^{(k)}(f_{i+2}^{(k)} - 2f_{i+1}^{(k)} + 2f_{i-1}^{(k)} - 2f_{i-2}^{(k)})$$

$$+ h^2 C_1(g_{i+1}^{(k)} - 2g_i^{(k)} + g_{i-1}^{(k)}). \tag{7}$$

Equations (4) are linearized in a similar manner. As a result, we obtain a system of equations for determining the sequences $\{g^{(k)}\}$, $\{\theta^{(k)}\}$, and $\{\varphi^{(k)}\}$:

$$C_2 g^{(k+1)''} + C_1(f^{(k)''} - 2g^{(k+1)}) - C_3\mathrm{Re}\,(f^{(k)}g^{(k+1)'} - f^{(k)'}g^{(k+1)}) = 0,$$

$$\theta^{(k+1)''} - \mathrm{Pe}_h(f^{(k)}\theta^{(k+1)'} - f^{(k)'}\theta^{(k+1)} - \mathrm{Ec}\,f^{(k)''2}) = 0, \tag{8}$$

$$\varphi^{(k+1)''} - \mathrm{Pe}_m(f^{(k)}\varphi^{(k+1)'} - f^{(k)'}\varphi^{(k+1)}) = 0.$$

The following iterative procedure is applied to obtain the numerical solution of systems (7) and (8).

1. An initial guess for $f^{(0)}$, $g^{(0)}$, $\theta^{(0)}$, and $\varphi^{(0)}$ is chosen to satisfy the boundary conditions (5).

2. The approximation $f^{(1)}$ is found by solving the linear system (7).

3. The derivatives in system (8) are replaced by finite differences, and the resultant algebraic system is solved to find the approximations $g^{(1)}$, $\theta^{(1)}$, and $\varphi^{(1)}$.

4. After the functions $f^{(1)}$, $g^{(1)}$, $\theta^{(1)}$, and $\varphi^{(1)}$ are determined, the procedure is repeated until the sequences $\{f^{(k)}\}$, $\{g^{(k)}\}$, $\{\theta^{(k)}\}$, and $\{\varphi^{(k)}\}$ converge to f, g, θ, and φ, respectively.

5. The calculations are terminated if the following inequalities are satisfied:

$$\max\,(\|f^{(k+1)} - f^{(k)}\|_{L_2},\ \|g^{(k+1)} - g^{(k)}\|_{L_2},\ \|\theta^{(k+1)} - \theta^{(k)}\|_{L_2},\ \|\varphi^{(k+1)} - \varphi^{(k)}\|_{L_2}) < 10^{-8}.$$

3. RESULTS AND DISCUSSION

The nonlinear system of coupled ordinary differential equations (3), (4) with the boundary conditions (5) is solved numerically by means of quasi-linearization for different values of the Reynolds number (Re), porosity parameter ε, micropolar material parameters C_1, C_2, and C_3, Peclet number (Pe_h), Eckert number (Ec), and Peclet number (Pe_m). We consider the effects of these parameters on the flow velocity $F'(\eta)$, microrotation $G(\eta)$, temperature $\theta(\eta)$, and concentration $\varphi(\eta)$, as well as on $f''(\pm1)$, $\theta'(\pm1)$, and $\varphi'(\pm1)$. The step of the dimensionless coordinate η is adjusted in such a way that the flow velocity, microrotation, temperature, and concentration profiles demonstrate asymptotic behaviors. The numerical results for different steps of η are listed in Table 1.

The values of the shear stresses $f''(-1)$ and $f''(1)$, heat transfer rates $\theta'(-1)$ and $\theta'(1)$, and mass transfer rates $\varphi'(-1)$ and $\varphi'(1)$ on both walls of the channel for $\varepsilon = 2.5$, $C_1 = 4$, $C_2 = 3$, $C_3 = 2$, $\mathrm{Pe}_h = 4$, $\mathrm{Ec} = 5$, $\mathrm{Pe}_m = 6$,

Table 1. Dimensionless temperatures $\theta(\eta)$ for $\mathrm{Re} = 10$, $\varepsilon = 2.5$, $C_1 = 4$, $C_2 = 3$, $C_3 = 2$, $\mathrm{Pe}_h = 4$, $\mathrm{Ec} = 5$, $\mathrm{Pe}_m = 6$, and different values of η and h

η	θ		
	$h = 0.01$	$h = 0.005$	$h = 0.0025$
−0.8	4.623886	4.623075	4.622887
−0.4	5.473856	5.473752	5.473746
0	3.923333	3.923930	3.924093
0.4	5.014426	5.014323	5.014316
0.8	3.758809	3.757999	3.757811

Table 2. Shear stresses and heat and mass transfer rates for $\varepsilon = 2.5$, $C_1 = 4$, $C_2 = 3$, $C_3 = 2$, $\mathrm{Pe}_h = 4$, $\mathrm{Ec} = 5$, $\mathrm{Pe}_m = 6$, and different values of Re

Re	$f''(-1)$	$\theta'(-1)$	$\varphi'(-1)$	$f''(1)$	$\theta'(1)$	$\varphi'(1)$
6	−2.9171	25.3783	−0.3865	2.9171	−25.8847	−0.004496
12	−2.7226	23.8979	−0.3740	2.7226	−24.3923	−0.004419
18	−2.6037	22.9303	−0.3654	2.6037	−23.4165	−0.004364
24	−2.5277	22.2763	−0.3595	2.5277	−22.7565	−0.004325
30	−2.4763	21.8165	−0.3552	2.4763	−22.2925	−0.004297

Table 3. Shear stresses and heat and mass transfer rates for $C_1 = 4$, $C_2 = 3$, $C_3 = 2$, $\mathrm{Pe}_h = 4$, $\mathrm{Ec} = 5$, $\mathrm{Pe}_m = 6$, $\mathrm{Re} = 10$, and different values of ε

ε	$f''(-1)$	$\theta'(-1)$	$\varphi'(-1)$	$f''(1)$	$\theta'(1)$	$\varphi'(1)$
9	−3.4462	29.8477	−0.4197	3.4462	−30.3856	−0.00470
18	−4.2297	37.0049	−0.4634	4.2297	−37.5836	−0.00498
27	−4.8982	43.5481	−0.4967	4.8982	−44.1574	−0.00520
36	−5.4853	49.5547	−0.5232	5.4853	−50.1879	−0.00537
45	−6.0116	55.1120	−0.5450	6.0116	−55.7648	−0.00551

Table 4. Shear stresses and heat and mass transfer rates for $\mathrm{Re} = -6$, $\varepsilon = 2.5$, $\mathrm{Pe}_h = 4$, $\mathrm{Ec} = 5$, $\mathrm{Pe}_m = 6$, and different values of C_1, C_2, and C_3

No.	Fluid parameters	$f''(-1)$	$\theta'(-1)$	$\varphi'(-1)$	$f''(1)$	$\theta'(1)$	$\varphi'(1)$
1	$C_1 = C_2 = C_3 = 0$ (Newtonian fluid)	−9.3689	88.2389	−0.6350	9.3689	−88.9670	−0.006 02
2	$C_1 = 0.6$, $C_2 = 0.8$, $C_3 = 0.6$	−6.2452	53.7636	−0.5366	6.2452	−54.4063	−0.00540
3	$C_1 = 1.2$, $C_2 = 1.2$, $C_3 = 0.9$	−5.0668	42.5491	−0.4904	5.0668	−43.1507	−0.00511
4	$C_1 = 1.8$, $C_2 = 1.6$, $C_3 = 1.2$	−4.5051	37.5985	−0.4660	4.5051	−38.1780	−0.00496
5	$C_1 = 2.4$, $C_2 = 2.0$, $C_3 = 1.5$	−4.1889	34.9254	−0.4513	4.1889	−35.4916	−0.00487

and different Reynolds numbers are listed in Table 2. The same parameters for $\mathrm{Re} = 10$, $C_1 = 4$, $C_2 = 3$, $C_3 = 2$, $\mathrm{Pe}_h = 4$, $\mathrm{Ec} = 5$, $\mathrm{Pe}_m = 6$, and different values of the porosity parameter ε are summarized in Table 3. The same parameters for $\mathrm{Re} = -6$, $\varepsilon = 2.5$, $\mathrm{Pe}_h = 4$, $\mathrm{Ec} = 5$, $\mathrm{Pe}_m = 6$, and different values of the micropolar material parameters C_1, C_2, and C_3 are listed in Table 4.

The heat and mass transfer rates for $\mathrm{Re} = 10$, $\varepsilon = 2.5$, $C_1 = 4$, $C_2 = 3$, $C_3 = 2$, and different values of Pe_h, Ec, and Pe_m are provided in Tables 5–7.

The Reynolds number produces practically no effect on the shear stresses $f''(-1)$ and $f''(1)$, heat transfer rates $\theta'(-1)$ and $\theta'(1)$, and mass transfer rate $\varphi'(-1)$ and $\varphi'(1)$ (see Table 2). As the porosity parameter increases, the shear stresses $f''(-1)$ and $f''(1)$, heat transfer rates $\theta'(-1)$ and $\theta'(1)$, and mass transfer rates $\varphi'(-1)$ and $\varphi'(1)$ increase. The values of $\theta'(-1)$ and $\theta'(1)$ on both walls of the channel increase with increasing Peclet number Pe_h and Eckert number Ec. With an increase in the Peclet number Pe_m, the mass transfer rate increases on the upper wall of the channel and decreases on the lower wall (see Table 7).

Table 5. Heat transfer rates for $\mathrm{Re} = 10$, $\varepsilon = 2.5$, $C_1 = 4$, $C_2 = 3$, $C_3 = 2$, $\mathrm{Ec} = 5$, $\mathrm{Pe}_m = 6$, and different values of Pe_h

Pe_h	$\theta'(-1)$	$\theta'(1)$
0.2	2.1858	−3.1460
0.4	4.4931	−5.4157
0.6	6.5229	−7.4098
0.8	8.3385	−9.1917
1.0	9.9824	−10.8036

Table 6. Heat transfer rates for $\mathrm{Re} = 10$, $\varepsilon = 2.5$, $C_1 = 4$, $C_2 = 3$, $C_3 = 2$, $\mathrm{Pe}_h = 4$, $\mathrm{Pe}_m = 6$, and different values of Ec

Ec	$\theta'(-1)$	$\theta'(1)$
0.3	0.4157	−1.1005
0.6	1.4380	−2.1227
0.9	2.4602	−3.1449
1.2	3.4824	−4.1672
1.5	4.5047	−5.1894

Table 7. Mass transfer rates for $\mathrm{Re} = 10$, $\varepsilon = 2.5$, $C_1 = 4$, $C_2 = 3$, $C_3 = 2$, $\mathrm{Pe}_h = 4$, $\mathrm{Ec} = 5$, and different values of Pe_m

Pe_m	$\varphi'(-1)$	$\varphi'(1)$
0	−0.5000	−0.4999
0.3	−0.5850	−0.3560
0.6	−0.6247	−0.2621
0.9	−0.6395	−0.1974
1.2	−0.6397	−0.1512

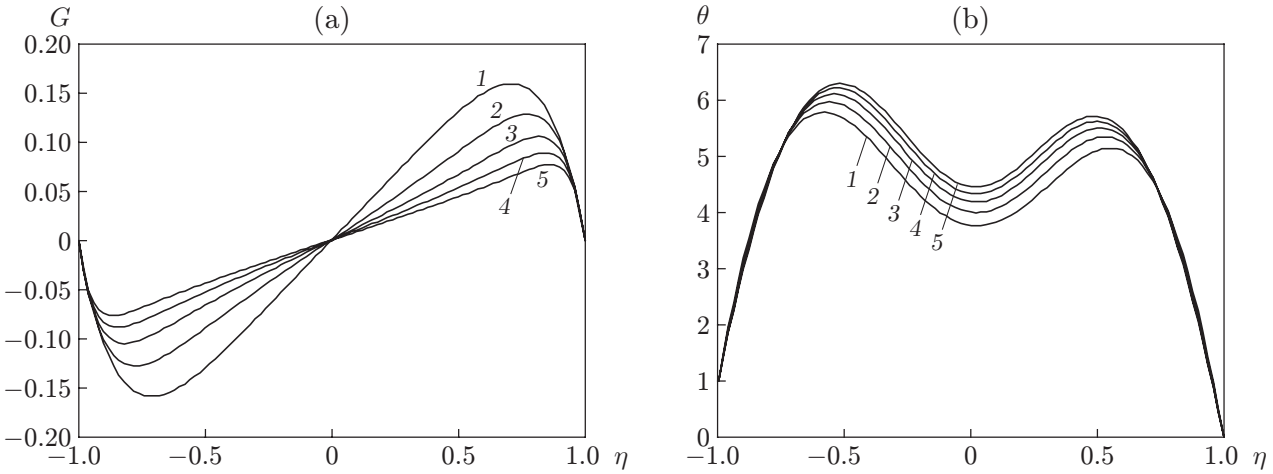

Fig. 2. Dependences $G(\eta)$ (a) and $\theta(\eta)$ (b) for $\varepsilon = 2.5$, $C_1 = 4$, $C_2 = 3$, $C_3 = 2$, $\mathrm{Pe}_h = 4$, $\mathrm{Ec} = 5$, $\mathrm{Pe}_m = 6$, and different values of Re: $\mathrm{Re} = 6$ (*1*), 12 (*2*), 18 (*3*), 24 (*4*), and 30 (*5*).

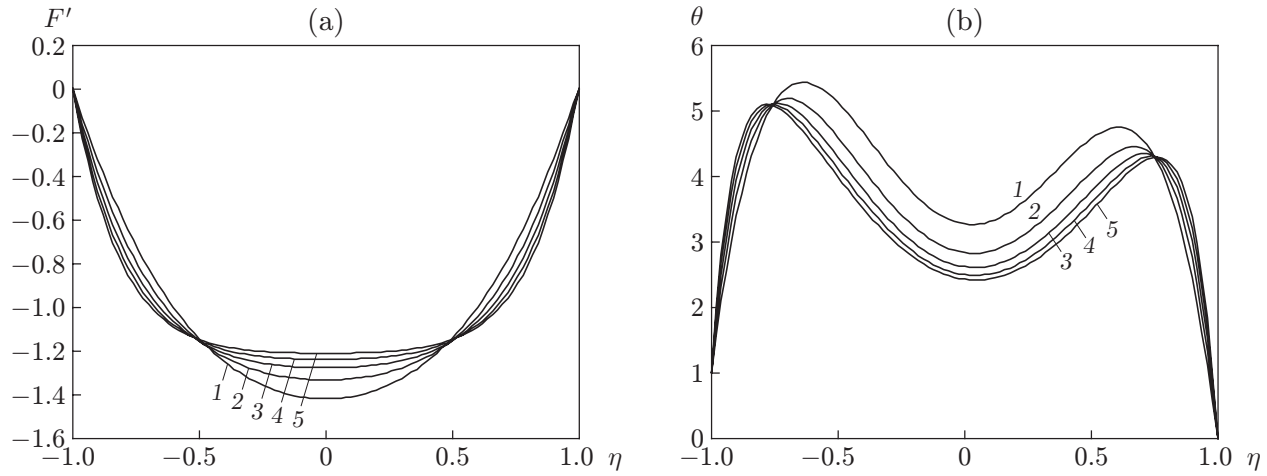

Fig. 3. Dependences $F'(\eta)$ (a) and $\theta(\eta)$ (b) for Re = 10, $C_1 = 4$, $C_2 = 3$, $C_3 = 2$, $\mathrm{Pe}_h = 4$, Ec = 5, $\mathrm{Pe}_m = 6$, and different values of ε: $\varepsilon = 9$ (*1*), 18 (*2*), 27 (*3*), 36 (*4*), and 45 (*5*).

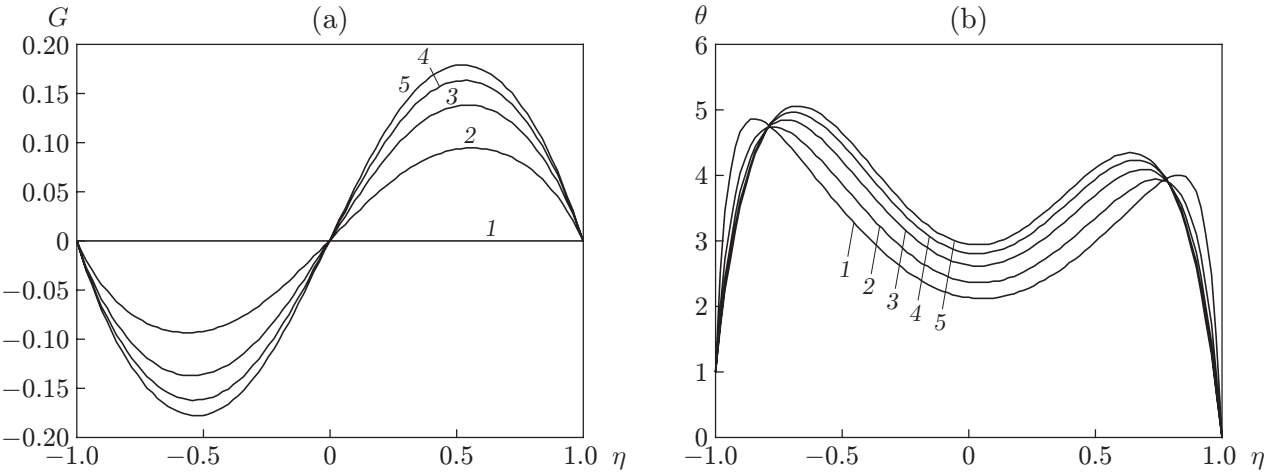

Fig. 4. Dependences $G(\eta)$ (a) and $\theta(\eta)$ (b) for Re = −6, $\varepsilon = 2.5$, $\mathrm{Pe}_h = 4$, Ec = 5, $\mathrm{Pe}_m = 6$, and different parameters of the fluid (see Table 4): curves *1*–*5* show the data for fluid Nos. 1–5, respectively.

Figure 2 show that an increase in the Reynolds number leads to a decrease in the microrotation profile $G(\eta)$ and to an increase in temperature on both walls of the channel. However, the velocity and concentration are almost independent of the Reynolds number.

The streamwise velocity F' and the temperature θ are displayed in Fig. 3 as functions of the coordinate η for several values of the porosity parameter ε. Figure 4 shows the functions $G(\eta)$ and $\theta(\eta)$ for different values of the micropolar material parameters C_1, C_2, and C_3 (see Table 4). The results of Fig. 3 designate that the flow velocity and temperature decrease with an increase in the porosity parameter. Figure 5 displays the curves of the temperature θ as a function of the coordinate η for different values of the Peclet number Pe_h and Eckert number Ec. It is seen that the temperature profiles rise up with an increase in both parameters. The concentration decreases with an increase in the Peclet number Pe_m (Fig. 6).

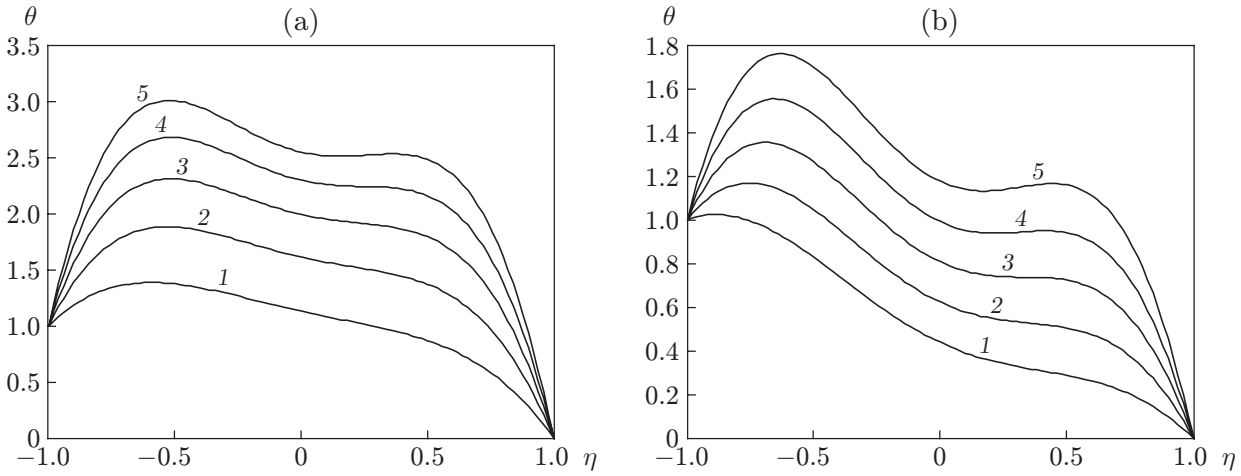

Fig. 5. Dependences $\theta(\eta)$ for Re = 10, $\varepsilon = 2.5$, $C_1 = 4$, $C_2 = 3$, $C_3 = 2$, $\mathrm{Pe}_m = 6$, and different values of the Peclet number Pe_h (a) and Eckert number Ec (b): (a) Ec = 5 and $\mathrm{Pe}_h = 0.2$ (*1*), 0.4 (*2*), 0.6 (*3*), 0.8 (*4*), and 1.0 (*5*); (b) $\mathrm{Pe}_h = 2$ and Ec = 0.3 (*1*), 0.6 (*2*), 0.9 (*3*), 1.2 (*4*), and 1.5 (*5*).

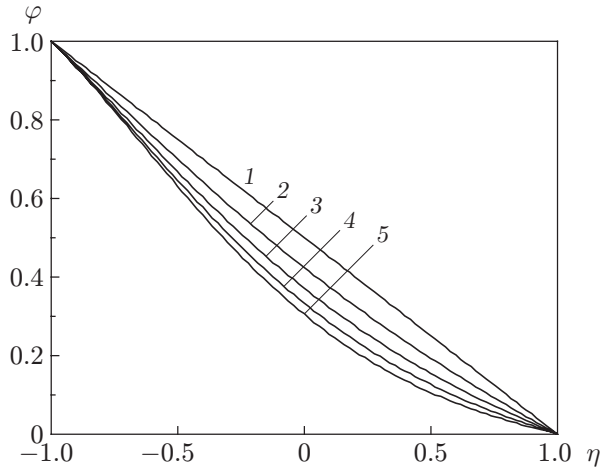

Fig. 6. Dependences $\varphi(\eta)$ for Re = 10, $\varepsilon = 2.5$, $C_1 = 4$, $C_2 = 3$, $C_3 = 2$, $\mathrm{Pe}_h = 4$, Ec = 5, and different values of Pe_m: $\mathrm{Pe}_m = 0$ (*1*), 0.3 (*2*), 0.6 (*3*), 0.9 (*4*), and 1.2 (*5*).

CONCLUSIONS

A laminar flow of a micropolar fluid through a resistive porous medium in a channel with plane walls is considered with allowance for viscous dissipation. By using suitable similarity variables, the system of nonlinear partial differential equations is reduced to coupled ordinary differential equations, which are solved numerically by means of quasi-linearization. The following conclusions are drawn. An increase in the Reynolds number and micropolar material parameters leads to reduction of the skin friction coefficient and heat and mass transfer rates on both the lower and upper walls of the channel. An increase in the micropolar material parameters tends to increase the flow velocity, microrotation, and temperature, while an increase in the porosity parameter produces the opposite effect. An increase in both the Eckert number and the Peclet number for the diffusion of heat leads to enhancement of the heat transfer rate on both walls of the channel.

REFERENCES

1. A. C. Eringen, "Theory of Micropolar Fluids," J. Math. Mech. **16**, 1–18 (1966).
2. A. C. Eringen, "Theory of Thermo-Microfluids," J. Math. Anal. Appl. **38**, 480–496 (1972).
3. T. Ariman, M. A. Turk, and N. D. Sylvester, "Microcontinuum Fluids Mechanics—A Review," Int. J. Eng. Sci. **11**, 905–930 (1973).
4. T. Ariman, M. A. Turk, and D. S. Nicholas, "Applications of Microcontinuum Fluid Mechanics," Int. J. Eng. Sci. **12**, 273–293 (1974).
5. Z. Ziabakhsh and G. Domairry, "Homotopy Analysis Solution of Micro-Polar Flow in a Porous Channel with Heat Mass Transfer," Adv. Theor. Appl. Mech. **1**, 79–94 (2008).
6. A. Mirzaaghaian and D. D. Ganji, "Application of Differential Transformation Method in Micropolar Fluid Flow and Heat Transfer Through Permeable Walls," Alexandria Eng. J. **55**, 2183–2191 (2016).
7. K. Ali and M. Ashraf, "Numerical Simulation of the Micropolar Fluid Flow and Heat Transfer in a Channel with a Shrinking and a Stationary Wall," J. Theor. Appl. Mech. **52** (2), 557–569 (2014).
8. M. Fakour, A. Vahabzadeh, D. D. Ganji, and M. Hatami, "Analytical Study of Micropolar Fluid Flow and Heat Transfer in a Channel with Permeable Walls," J. Molecular Liq. **204**, 198–204 (2015).
9. H. Mirgolbabaee, S. T. Ledari, and D. D. Ganji, "Semi-Analytical Investigation on Micropolar Fluid Flow and Heat Transfer in a Permeable Channel using AGM," J. Assoc. Arab Univ. Basic Appl. Sci. **24**, 213–222 (2017).
10. M. Sheikholeslami, M. Hatami, and D. D. Ganji, "Micropolar Fluid Flow and Heat Transfer in a Permeable Channel Using Analytical Method," J. Molecular Liq. **194**, 30–36 (2014).
11. Xinhui Si, Liancun Zheng, Ping Lin, et al., "Flow and Heat Transfer of a Micropolar Fluid in a Porous Channel with Expanding or Contracting Walls," Int. J. Heat Mass Transfer **67**, 885–895 (2013).
12. P. O. Nwabuzor, A. T. Ngiangia, and E. O. Chukwuocha, "MHD Flow of Micropolar Fluid in a Porous Medium Provoked by Heat Function and Radiation," Asian J. Phys. Chem. Sci. **6** (2), 1–20 (2018).
13. M. Ashraf, M. A. Kamal, and K. S. Syed, "Numerical Study of Asymmetric Laminar Flow of Micropolar Fluids in a Porous Channel," Comput. Fluids **38** (10), 1895–1902 (2009).
14. G. M. Shrestha and R. M. Terrill, "Laminar Flow with Large Injection Through Parallel and Uniformly Porous Walls of Different Permeability," Quart. J. Mech. Appl. Math. **21** (4), 413–432 (1968).